

# Jet Cross Sections in $\gamma^*\gamma$ -Scattering at $e^+e^-$ Colliders in NLO QCD

B. Pötter<sup>a\*</sup>

<sup>a</sup>II. Institut für Theoretische Physik, Universität Hamburg, Luruper Chaussee 149, D-22761 Hamburg, Germany (e-mail: poetter@mail.desy.de)

Recent results from NLO QCD calculations for inclusive jet cross sections in  $\gamma^*\gamma$ -scattering at  $e^+e^-$  colliders, especially for LEP, are reported. The virtuality  $Q^2$  of the virtual photon is non-zero and can be unlimited large. The virtuality of the second photon is zero and the spectrum is calculated with the Weizsäcker-Williams approximation. Four components of the cross sections have to be distinguished, involving direct and resolved real and virtual photon contributions. Since  $Q^2$  is non-zero, the virtual photon structure function is needed to calculate the contributions involving a resolved virtual photon.

## 1. Introduction

Jet production in  $\gamma\gamma$ -scattering is an interesting field, both to study perturbative QCD and to obtain information about the partonic structure of the photon. Jet production from two photons can be obtained at  $e^+e^-$ -colliders as a subprocess to the reaction  $e^+e^- \rightarrow e^+e^- + X$ . The leptons both radiate photons that, in the simplest case, couple to a quark-antiquark pair which produces jets with high  $E_T$  in the final state. In the case that both leptons disappear undetected in the beam pipe the photons are quasi-real. This case has been studied at TRISTAN [1] and LEP [2] experiments. The presence of a large scale ( $E_T$ ) allows perturbative QCD calculations. These have been performed [3–6] and the agreement of the predictions with experimental data is good (see e.g. [7]). Recently it has become possible to detect one of the leptons to perform a single-tag experiment [8]. The detection of the lepton allows to reconstruct the virtuality ( $Q^2$ ) of the radiated photon and it is thus possible to obtain data on jet production for the case of scattering of virtual on real photons.

It is well-known that the real photon can not only couple directly to the charge of the bare

quarks but can also fluctuate into a bound state and thus serve as a source of quarks and gluons. This resolved component is described by a parton distribution function (PDF) of the real photon. Thus, the scattering of photons also provides a possibility to study the parton contents of the photon. The resolved component of the virtual photon deviates from that of the real photon in that it has a  $Q^2$ -dependence. At large  $Q^2$  the resolved component of the virtual photon is believed to be negligible. Since so far only limited data exist for the structure of the virtual photon [9], the modeling of the  $Q^2$ -behaviour of the virtual photon PDF is still rather ambiguous. Mainly two LO parametrizations of the virtual photon PDF exist, namely those of Glück, Reya and Stratmann [10], and of Schuler and Sjöstrand [11].

Cross sections have been calculated for  $\gamma^*\gamma$ -scattering at LO accuracy some time ago [12], but LO calculations suffer from rather large scale and scheme dependences. Thus, it is desirable to perform these calculations in NLO, which has been achieved recently [13].

## 2. Partonic Cross Section in NLO QCD

We will consider  $e^+e^-$ -scattering cross sections with the  $\gamma^*\gamma$ -scattering subprocess

$$\gamma_a^*(Q^2) + \gamma_b(P^2 = 0) \rightarrow \text{jet}_1 + \text{jet}_2 + X \quad (1)$$

\*Supported by the Bundesministerium für Forschung und Technologie, Bonn, Germany, under Contract 05 7 HH 92P (0), and by EEC Program *Human Capital and Mobility* through Network *Physics at High Energy Colliders* under Contract CHRX-CT93-0357 (DG12 COMA).

The interaction of a virtual with a real photon can happen in four different ways, depending on whether the photon interacts directly or resolved, which is depicted in Fig. 1. The variables  $y_a, y_b$  in the following describe the momentum fraction of the photon  $a, b$  in the electron and  $x_a, x_b$  describes the momentum fraction of the parton in the photon  $a, b$ .

Taking into account both the transverse and longitudinal polarizations of the virtual photon, the cross section  $d\sigma_{e^+e^-}$  for  $e^+e^-$ -scattering is conveniently written as the convolution

$$\frac{d\sigma_{e^+e^-}}{dQ^2 dy_a dy_b} = \sum_{a,b} \int dx_a dx_b F_{\gamma/e^-}(y_b) f_{b/\gamma}(x_b) \times \frac{\alpha}{2\pi Q^2} \left[ \frac{1 + (1 - y_a)^2}{y_a} f_{a/\gamma^*}^U(x_a) d\sigma_{ab} + \frac{2(1 - y_a)}{y_a} f_{a/\gamma^*}^L(x_a) d\sigma_{ab} \right] \quad (2)$$

The PDF's of the real and the virtual photon are  $f_{b/\gamma}(x_b)$  and  $f_{a/\gamma^*}^{U,L}(x_a)$ , respectively, where  $U$  and  $L$  denote the unpolarized and longitudinally polarized photon contributions, respectively. The direct photon interactions are included in formula (2) through delta functions. For the direct virtual photon one has the relation  $f_{a/\gamma^*}^{U,L} d\sigma_{ab} = \delta(1 - x_a) d\sigma_{\gamma^* b}^{U,L}$ , whereas for the direct real photon the relation is  $f_{a/\gamma} d\sigma_{ab} = \delta(1 - x_b) d\sigma_{\gamma b}$ , where  $d\sigma_{ab}$  refers to the partonic cross section. The function  $F_{\gamma/e^-}(y_b)$  describes the spectrum of the real photons emitted from the electron according

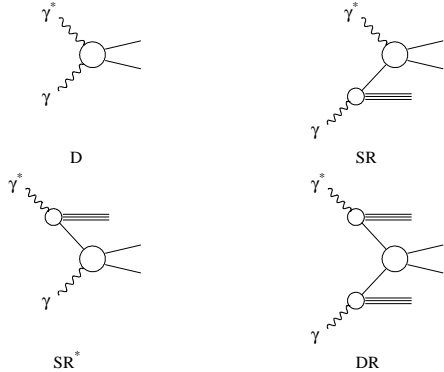


Figure 1. The four different interaction modes in  $\gamma^*\gamma$ -scattering.

to the Weizsäcker-Williams approximation [14].

The partonic cross sections in LO consist of two final state particles. The NLO corrections consist of the virtual and real corrections, which both exhibit characteristic divergencies. The real corrections for the different subprocesses D, SR, SR\* and DR have been calculated with the phase-space slicing method and are available in the literature in NLO [5,13,15]. The sum of real and virtual corrections is finite after factorization of singularities from the initial state. Of special importance here is the  $\gamma^* \rightarrow q\bar{q}$  splitting term. In the limit of the  $q\bar{q}$ -pair being collinear the logarithm

$$M = \ln \left( 1 + \frac{y_s s}{z Q^2} \right) P_{q \leftarrow \gamma}(z) \quad (3)$$

(where  $y_s$  is the phase-space-slicing parameter and  $s$  is the partonic cms energy) can be factorized from the cross section, which is singular for  $Q^2 = 0$ . This singularity is absorbed into the PDF of the virtual photon with virtuality  $Q^2$  in such a way that the  $\overline{\text{MS}}$  factorization result of the real photon is obtained in the limit  $Q^2 \rightarrow 0$  [16].

### 3. Results for Jet Cross Sections

The different subprocesses D, SR, SR\* and DR have been implemented into the computer program *JetViP* [17] which allows to calculate jet cross sections in  $\gamma^*\gamma$ -scattering using the Snowmass jet algorithm [18].

For producing our plots we assume kinematical conditions that will be encountered at LEP2, where the photons are emitted by colliding electrons and positrons, both having the energy of  $E_e = 83.25$  GeV. We choose the configuration, where the virtual photon travels in the positive  $z$ -direction. We consider only the  $\overline{\text{MS}}$ -GRS [10] parametrization of the photon PDF here. We use the PDF of GRS for both, the real and the virtual photon. We have set the number of flavors to  $N_f = 4$ , adding the contributions from photon-gluon fusion by fixed order perturbation theory. The renormalization and factorization scales are set equal, with  $\mu_R = M_\gamma = M_{\gamma^*} = E_T$ .

In Fig. 2 a and b the  $E_T$  spectra for the virtualities  $Q^2 = 0.058$  and  $1.0$  GeV $^2$  for the cross section  $d^3\sigma/dE_T d\eta dQ^2$  are shown, integrated over

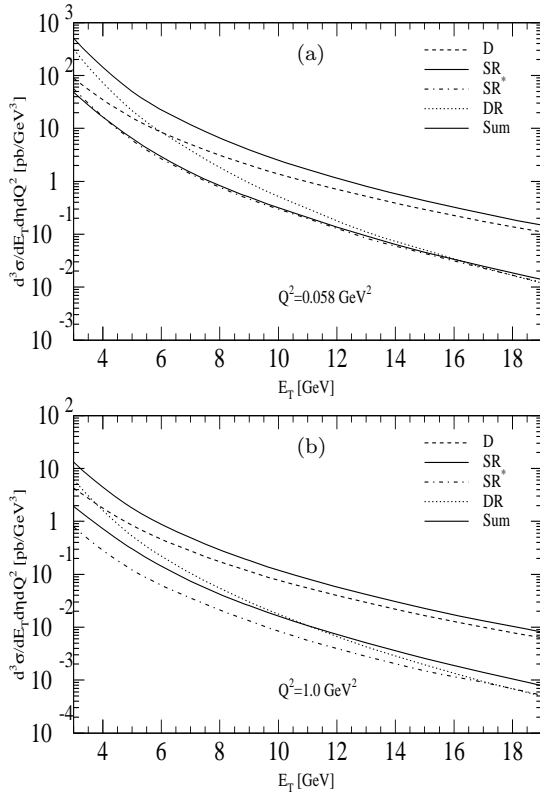


Figure 2. Single-jet inclusive cross section integrated over  $\eta \in [-2, 2]$ . The upper full curve is the sum of the D, SR, SR\* and the DR components. (a)  $Q^2 = 0.058 \text{ GeV}^2$ ; (b)  $Q^2 = 1.0 \text{ GeV}^2$ .

the interval  $-2 \leq \eta \leq 2$ . The value  $Q_{eff}^2 = 0.058 \text{ GeV}^2$  is chosen as to reproduce the  $Q^2 \simeq 0$  case. The SR (lower full) and SR\* (dash-dotted) curves coincide in Fig. 2 a, where the real photon is approximated by the integrated Weizsäcker-Williams formula and the virtual photon has the value of  $Q_{eff}^2$ . The full cross section (upper full curve) is dominated by the DR component in the small  $E_T$  range for the small  $Q^2$  value. For  $Q^2 = 1.0 \text{ GeV}^2$ , the DR and D contributions are of the same order around  $E_T = 4 \text{ GeV}$ , but the DR component falls off quickly for the higher  $E_T$ 's, leaving the D component as the dominant contribution. This is expected, since the point-like coupling of the photons is more important for larger  $E_T$  and  $Q^2$ . Since the virtual photon

contribution is suppressed for larger  $Q^2$  the SR\* contribution falls below the SR curve when going to higher values of  $Q^2$ . In all curves, both SR contributions do not play an important role for the full cross section. Of course, all contributions decrease with increasing  $Q^2$ .

We turn to the  $\eta$ -distribution of the single-jet cross section for fixed  $E_T = 10 \text{ GeV}$  between  $-2 \leq \eta \leq 2$  for the virtualities  $Q^2 = 0.058, 1, 5$  and  $9 \text{ GeV}^2$ , plotted in Fig. 3 a-d. The D and DR distributions for the lowest virtuality  $Q_{eff}^2$  are almost symmetric, because of the identical energies of the incoming leptons. The SR curve falls off for negative  $\eta$ , whereas the SR\* component is suppressed for positive  $\eta$ . Going to higher  $Q^2$  values, the D contribution stays more or less symmetric and dominates the full cross section, as we have already seen in Fig. 2 for the larger  $E_T$  values. The components containing contributions from the resolved virtual photon DR and SR\* fall off in the region of negative  $\eta$  so that they become more and more asymmetric. This is clear, since we have chosen the virtual photon to be incoming from the positive  $z$ -direction and the resolved virtual photon contribution is decreasing for higher virtualities. The DR and SR contributions are of the same magnitude in the negative  $\eta$  region and the DR component is dominant for the larger  $\eta$  values, where the resolved photon is more important. The same holds for the D and SR\* distributions in the negative  $\eta$  region, only here the D component is far more dominant than the SR\* component in the whole  $\eta$  region.

### Acknowledgements

I am grateful to G. Kramer for interesting discussions.

### REFERENCES

1. H. Hayashi et al., TOPAZ Collaboration, Phys. Lett. **B314** (1993) 149; B.J. Kim et al., AMY Collaboration, Phys. Lett. **B325** (1994) 248.
2. K. Ackerstaff et al., OPAL Collaboration, Z. Phys. **C73** (1997) 433.
3. P. Aurenche, J.-Ph. Guillet, M. Fontannaz, Y. Shimizu, J. Fujimoto, K. Kato, Progr. Theor.

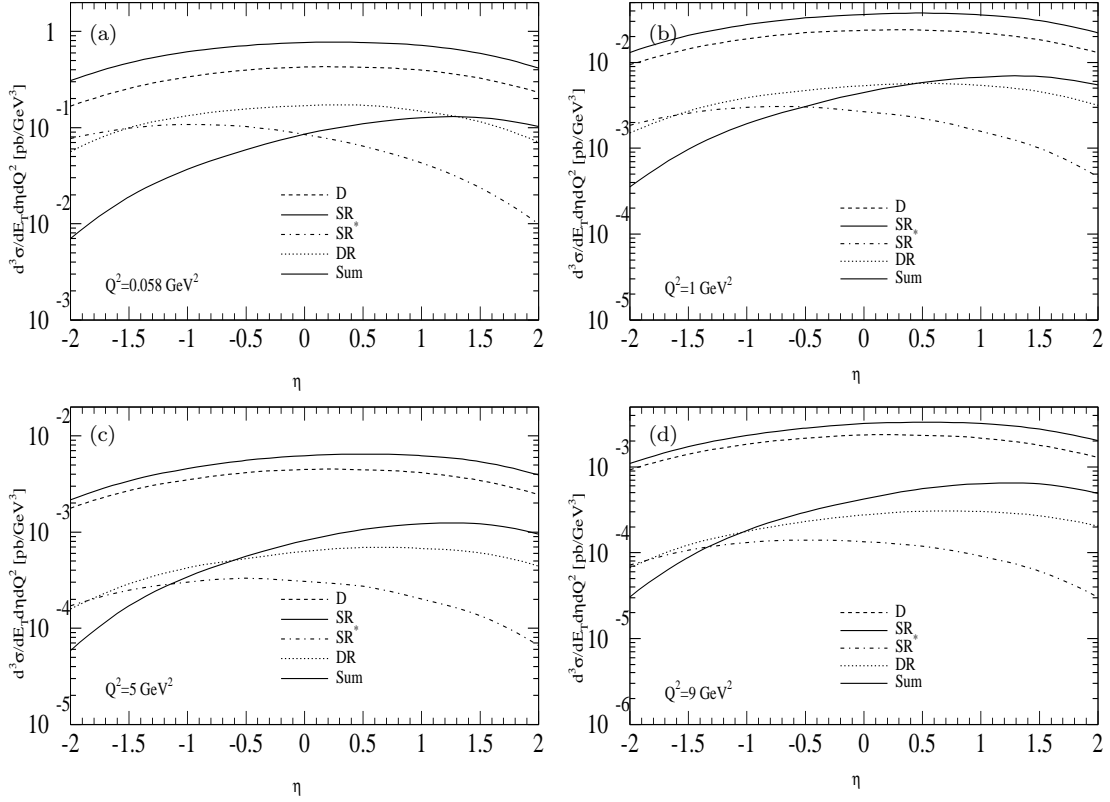


Figure 3. Single-jet inclusive cross section as a function of  $\eta$  for fixed  $E_T = 10$  GeV. The upper full curve is the sum of the D, SR,  $SR^*$  and the DR components. (a)  $Q^2 = 0.058$  GeV $^2$ ; (b)  $Q^2 = 0.5$  GeV $^2$ ; (c)  $Q^2 = 1.0$  GeV $^2$ ; (d)  $Q^2 = 9.0$  GeV $^2$ .

Phys. **92** (1994) 175.

4. L.E. Gordon, Nucl. Phys. **B419** (1994) 25.
5. T. Kleinwort, G. Kramer, Nucl. Phys. **B477** (1996) 3; M. Klasen, T. Kleinwort, G. Kramer, EPJ direct **1** (1998) 1.
6. T. Kleinwort, report DESY 96-165 (thesis).
7. T. Kleinwort, G. Kramer, Phys. Lett. **B370** (1996) 141; Z. Phys. **C75** (1997) 489.
8. J. Lauber (OPAL), G. Cowan (ALEPH), private communication.
9. Ch. Berger et al., PLUTO Collaboration, Phys. Lett. **B142** (1984) 119.
10. M. Glück, E. Reya, M. Stratmann, Phys. Rev. **D51** (1995) 3220.
11. G.A. Schuler, T. Sjöstrand, Z. Phys. **C68** (1995) 607; Phys. Lett. **B376** (1996) 193.
12. A.C. Bawa, W.J. Stirling, Z. Phys. **C57** (1993) 165.
13. B. Pötter, report DESY 97-138 [hep-ph/9707319] (thesis); B. Pötter, report DESY 98-052 [hep-ph/9805436].
14. C.F. v. Weizsäcker, Z. Phys. **88** (1934) 612; E.J. Williams, Kgl. Danske Vidensk. Selskab. Mat-Fiz. Medd. **13** (1935) N4.
15. D. Graudenz, Phys. Rev **D49** (1994) 3291.
16. M. Klasen, G. Kramer, B. Pötter, Eur. Phys. J. **C1** (1998) 261.
17. B. Pötter, JetViP 1.1, report DESY 98-071 [hep-ph/9806437].
18. J.E. Huth et al., Proc. of the 1990 DPF Summer Study on High Energy Physics, Snowmass, Colorado, edited by E.L. Berger, World Scientific, Singapore, 1992, p. 134.